POAC'11
Montréal, Canada

Proceedings of the 21st International Conference on
Port and Ocean Engineering under Arctic Conditions
July 10-14, 2011
Montréal, Canada

POAC11-038

ICE CRUSHING PRESSURE DISTRIBUTION AGAINST A COMPLIANT STIFFENED PANEL

Mauri Määttänen[1], Pieti Marjavaara[2], Sami Saarinen[3]
[1]Aalto University, Finland / NTNU, Norway
[2]VTT, Espoo, Finland
[3]Aker Arctic, Helsinki, Finland

ABSTRACT
Near full-scale ice crushing tests were conducted in Aker Arctic test basin in order to learn on the effects of stiffened plate compliance on the crushing pressure distribution. A 1:3 scale ratio test rig was designed to allow ice to be crushed in controlled conditions against a stiffened plate presenting a typical full size ship or offshore structure plating to withstand 60 cm thick level ice crushing loads. The target plate was instrumented both with strain gauges and a large tactile sensor for detailed load distribution measurement both directly against the plate surface and further through the stiffeners. The ice blocks to be crushed were manufactured in snow filled moulds by vacuum water impregnation to guarantee predictable model ice properties. Altogether 22 ice blocks were crushed while the varied test parameters were ice velocity and stiffener compliancy. The paper presents the test arrangements, instrumentation and major results. After the initial peak ice load failure well known line like contact sustained for the rest of each brittle crushing test. Contrary to expectations the plate compliance played no role in crushing pressure distribution. This differs from what is assumed in some ice rules, e.g. the highest pressure at the location of stiffeners. The implications of this finding are explained in the paper.

INRODUCTION
Ice crushing is present either as dominant or contributing factor in almost all ice failure modes in any ice-structure interaction scenario. However, regardless of over 50 years of research the true physics of ice crushing is not yet fully understood. Assume a case of straight ice edge hitting squarely a straight structural surface with ice velocity above the creep range. The initial even crushing pressure turns after the first ice failure into brittle non-simultaneous series of randomly in time and space varying ice failures at high local pressure at hot spots along the narrow line like contact line. The rest of the contact surface experiences only low ice pressures. The evolution from effective pressure, Korzhavin 1960, to the present level of understanding, Joensuu 1988, Jordaan et al. 2008, has been paved both with laboratory and full-scale measurements. In laboratory tests the surface of structure under crushing pressure has usually been very rigid. The real full-scale structures have variable compliance at the surface plates prone to ice action but the instrumentation has – due to practical reasons - been limited to provide accurate enough measurements on pressure distributions for understanding compliance effects.

A subtask in the Finnish joint industry project (STRUTSI, 2008-2010) was created to find out the effects of surface plating compliance to ice crushing pressure distributions in ship or offshore structures, and to provide detailed data for numerical model verification. The laboratory model tests presented in this paper were planned to be close to full-scale and to utilize specific instru-

mentation to capture the true compliance effects. The conducted test series produced new understanding about the ice crushing phenomena. More results of these tests are presented in Määttänen et al. (2011)

TEST SET-UP

The most reliable results could be achieved with full-scale tests in the nature but at high cost. This in mind a scale ratio of 1:3 was chosen to present a typical Baltic 60 cm thick ice by using a 20 cm thick model ice. The chosen scale ratio is an order of magnitude closer to the full scale than what is typical in most scale model tests. The crushing tests were conducted in Aker Arctic Test Basin in Helsinki. A loading rig, Fig. 1, was designed to allow the model ice block to be pushed at controlled velocity against the compliant instrumented surface plate. The ice block 200x700/800x1200 mm^3 is fixed to the sledge in the rig and lowered to normal freely floating ice level in the basin. A 1 MN hydraulic cylinder pushes the ice block from behind against the instrumented reinforced panel. The ends of the ice blocks facing the instruments are tapered 100 mm from both edges to promote the ice failure to start from the instrumented end.

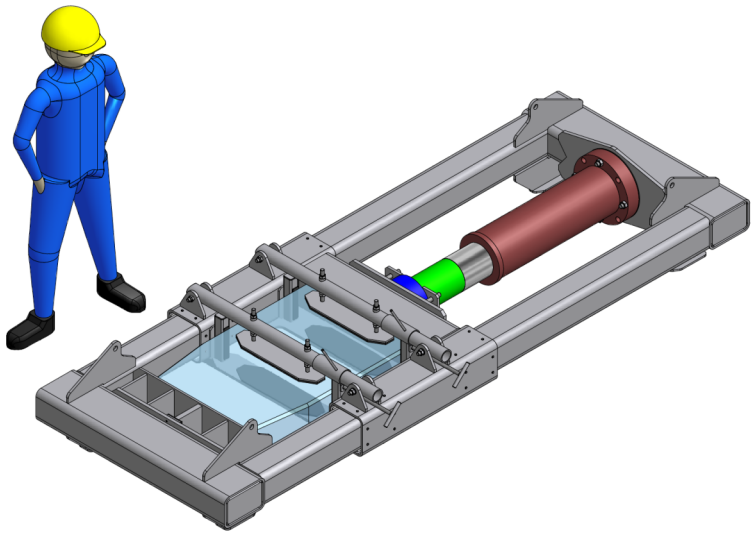

Figure 1. The test rig with hydraulic actuator, ice block and the instrumented plate.

The instrumented 12 mm thick plate for ice crushing was simulating in 1:3 ratio a ship or offshore structure surface steel plating at waterline with 600 mm spacing between rigid supporting stiffeners. In addition to the deflection of the surface plate in between the stiffeners, the compliance of the centre stiffener could be increased. In reference to the maximum plate deflection under constant pressure the compliance could be increased more than two orders of magnitude. In

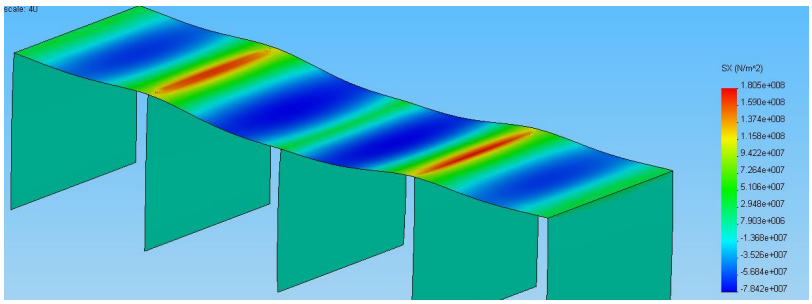

Figure 2. The instrumented reinforced plate FE-model. Load 1 MPa uniform pressure in the medium stiffness configuration at the centre.

reference to maximum plate deflection the displacements at 1 MPa constant pressure were 0.013 mm, 0.476 mm Fig. 2, and 2.12 mm for the three compliance settings.

INSTRUMENTATION

The instrumentation system included a load cell for the measurement of the total pushing force generated by the hydraulic cylinder. During the tests the friction force, while the sledge is moving at different velocities, was measured without ice in order to get the base value to be subtracted from the total pushing force. The ice velocity was continuously measured with a laser rangefinder for solving the ice velocity by derivation in time.

The surface plate and the supporting stiffeners had 24 strain gauges for measuring total load distribution and its paths from the contact surface to the rig. A large 482 mm wide and 207 mm high tactile sensor having a grid of 52 times 44 sensing elements (sensels), each 6.7x3.0 mm^2, was installed on the front surface of the reinforced plate to measure the direct ice pressure during crushing. The tactile sensor height exceeded ice thickness but the width was less than the width of the oncoming ice block. To protect the sensing elements from damage due to direct ice action it was covered with a 0.5 mm thick steel plate, Fig. 3. Comparing to the bending stiffness of the plate itself the effect of protection plate is insignificant. Another concern was how much the protective steel sheet would spread the width of the line like contact – the narrow high pressure zone at the contact area. The plate on elastic analysis model verified that the spreading effect would be less than the sensel height 3 mm.

Figure 3. The tactile sensor protection plate. The plotted rectangle is the true location of the sensing area. The three vertical lines are the locations of stiffeners and give guidance to their positions in Fig. 5 and 7.

Two computer systems recorded the measurement data: one was for strain gauges, load cell, and laser distance, and the other solely for the tactile sensor. In addition the whole crushing action against the target plate was stored on video. A common timing pulse synchronized all these measurements.

MODEL ICE

In order to utilize scale model data for full-scale structural design the geometric similitude of ice failure patterns and scalable mechanical ice properties to structural dimensions are required. The model ice shall be homogeneous and repeatedly produce as close as possible the same ice failure processes as in the full scale. To optimize the accuracy and cost a scale ratio 1:3 was chosen for these tests

Growing a 20 cm thick ice sheet in the test basin is unfeasible and cutting test ice blocks from natural sea ice would inherit uncontrolled variability to ice properties. The choice was to manufacture the test ice in moulds, first fully packing them with snow, sucking in low salinity water under vacuum to flood the cavities within snow crystals, and by controlling the freezing front to proceed uniformly from bottom to top. The mould inner dimensions were 0.80x1.40x0.19 m^3. The mould length was made longer than what was needed in a crushing test. The extra length was used for ice compressive and flexural strength index strength samples.

After complete freezing the ice blocks were cut to the final plan view by first cutting a 200 mm slab from one end for index strength tests and then tapering the forward end to 700 mm width, Fig 3. Then the ready for testing ice blocks were stored in a freezer container at -20 ºC while the moulds were re-used for manufacturing more ice test blocks.

The index strength tests proved that the model ice properties were good. The average density of 860 kg/m^3 with the standard deviation of only 1.7 % indicates the even quality of ice blocks and that the porosity due to entrapped air within snow – the seeding crystals - is minimal. The compressive index strength at -10 °C was 2,6 MPa with 22 % standard deviation and flexural strength up to 0.9 MPa. Due to amplifier failure only the first of bending tests were reliable. The index strength data was at the expected range with the chosen scale ratio 1:3.

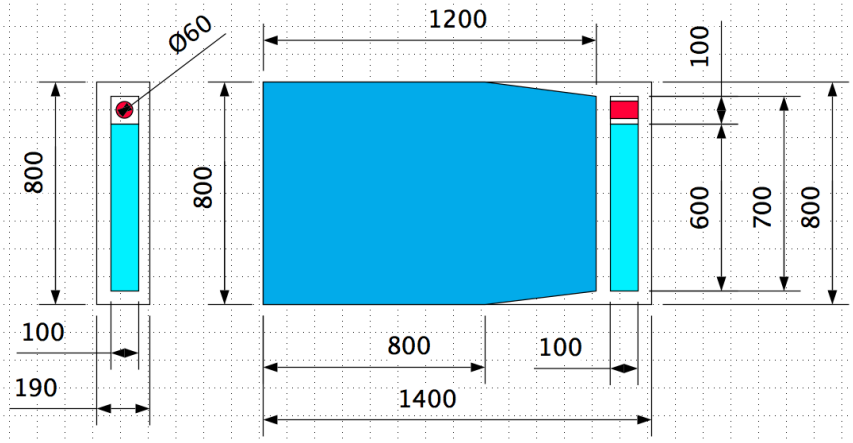

Figure 4. The dimensions (mm) of the test block and the locations of index strength ice samples.

RUNNING A TEST

The dress rehearsal tests with three ice blocks half a year before the real tests indicated that crushing test with more than 10 ice blocks can be carried trough in a day. The planned 22 test matrix cases were scheduled for two days and this was also realized in actual tests. The temperature of the storage container was increased to -5 °C two days before the tests. The desired temperature range for the ice blocks during the tests was from -3 to -5 °C. When the ice block was taken out from the storage it took normally 15 to 30 minutes before crushing could be started. Initial steps were the measurement of true dimensions of the block and its temperature at the depths of 20 mm and 90 mm at the centre part of the block. This took place in the preparation area where air temperature was from +10 to +15 °C. Then the ice block was lowered into test basin water at -1 °C, floated into the test rig and fixed to the sledge. The sledge was driven to have a slight contact to the tactile sensor protection plate. A handsaw was used to cut out the protruding spots of the ice edge while the protection plate acted as planar guide to the handsaw. The tactile sensor pressure map after a sawing phase and new ice edge contact indicated how smooth the surface was and whether further smoothing was needed.

The ice driving velocity was adjusted to the planned value of each test. First the data logging computers and the video were set ready to go and turned on. Then the synchronizing signal was triggered and thereafter the hydraulics was turned on to push the ice block at constant velocity. The crushing test stroke was typically 400 mm and depending on the chosen velocity the test duration varied from about 10 to 300 s. After the test the sledge was driven back and the final ice edge profile was inspected and photographed. The best way was to remove the ice block from the sledge and turn it into vertical floating position with the crushed edge upwards in the air for inspection.

The total time, ice block was first at elevated room temperature and thereafter in freezing water before testing, was less than half an hour from taking it out from the storage container. Considering the thermal inertia, only a relatively thin surface layer of the ice block experienced warming while the core of the ice block remained at the temperature that was measured just before immersing it into the test basin.

RESULTS

The total number of ice crushing tests was 22 at three different plate compliance settings and at three ice velocity ranges with ice failure modes at creep, transition, and brittle modes. The creep mode below 0,2 mm/s ice velocity was completely distinct from the rest having continuous contact along the whole ice edge: quite evenly distributed pressure, no initial peak load but a gradual load increase, which after a while started to slowly decrease due to tertiary creep effects, Fig. 5 and 6.

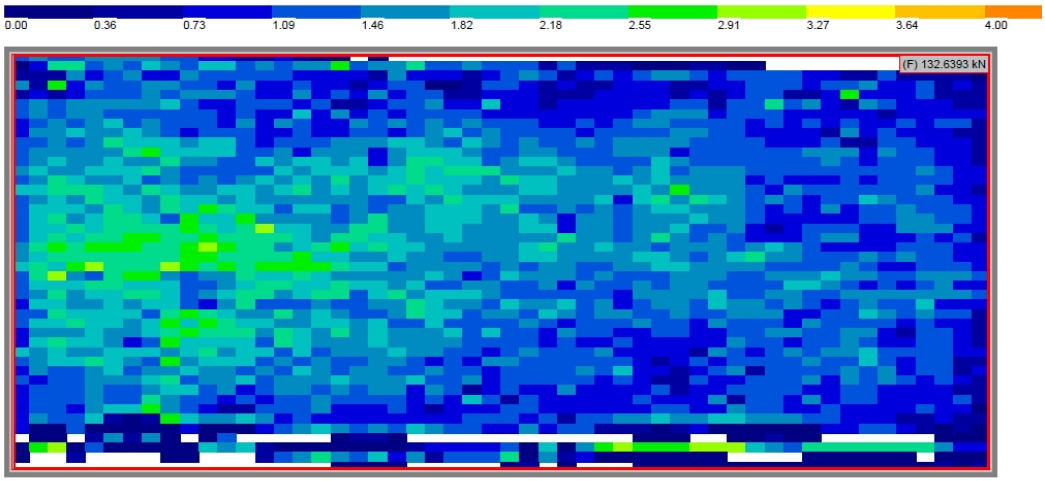

Figure 5. Typical pressure distribution in creep tests (here v=0.03 mm/s)

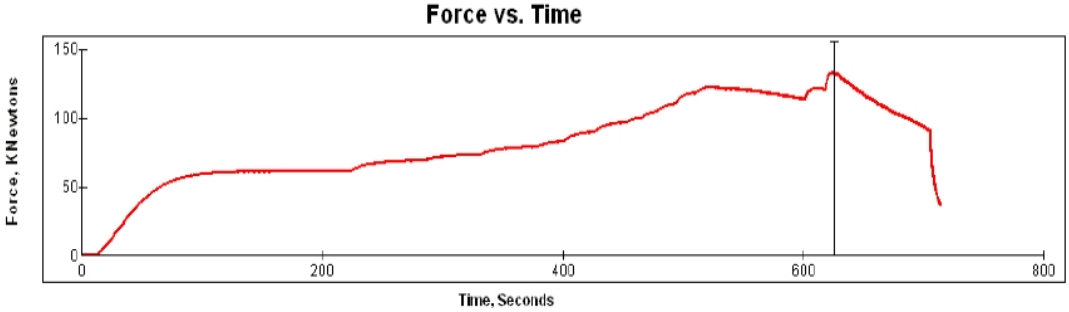

Figure 6. Typical load history at creep range. Starting velocity 0.03 mm/s, with small velocity step increases at about 220 s, 600 s, and 615 s.

Tests both at transitional and true brittle velocities produced similar ice load histories, first high initial peak load and thereafter a significant reduction, line like contact, and randomly varying load, Fig, 7 and 8. During the initial peak load the ice pressure was relatively constant along the whole contact surface, but in continuous crushing - after the peak load – a high pressure persisted only at narrow line like contact close to the mid section of ice thickness. These findings are similar to earlier crushing test results with tactile sensors, Tageuchi et al. 1997, Sodhi et al. 2001, Frederking 2004.

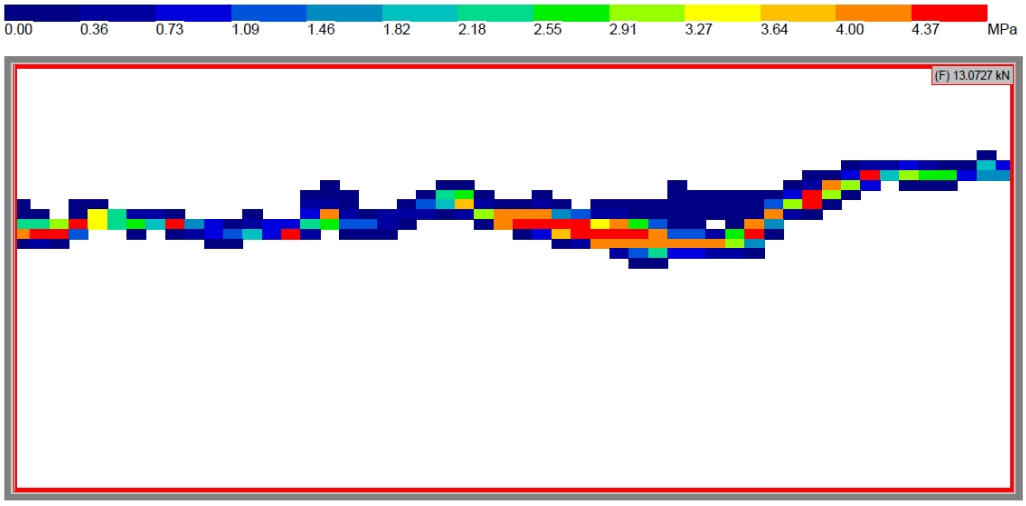

Figure 7. Pressure distribution at continuous crushing at 6.1 mm/s ice velocity with persistent line like contact.

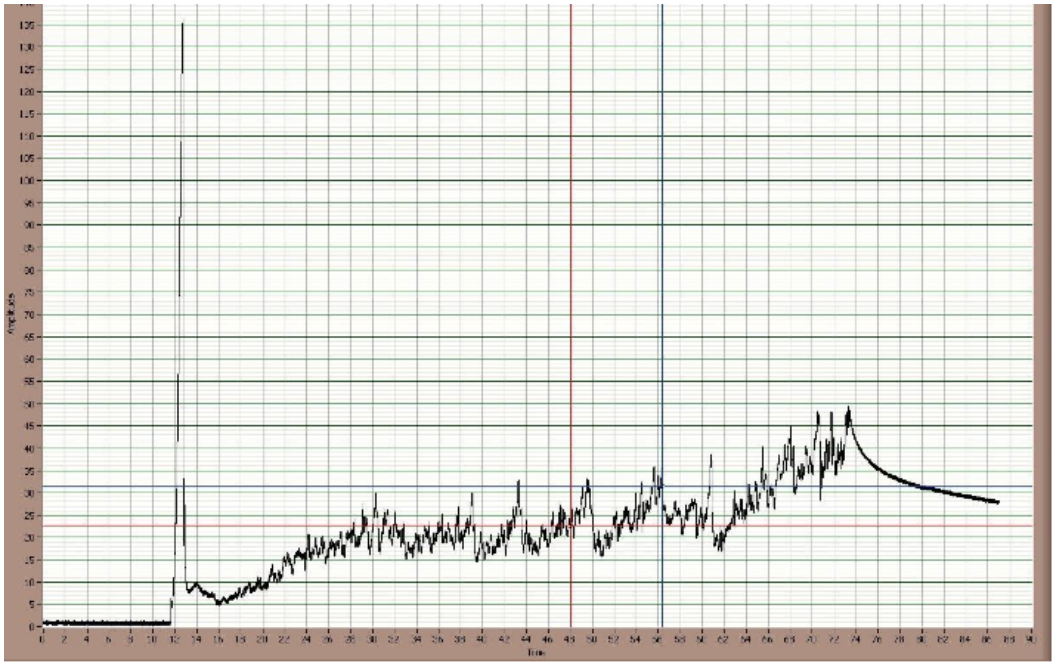

Figure 8. A ice crushing load history at 6.1 mm/s ice velocity.

With ice velocities above 1 mm/s the ice failure mode presented brittle behaviour and thereafter remained similar even at highest velocities of 18 mm/s. When the strain rates are calculated by dividing the ice velocity with the length of the ice block the low velocity strain rate $0.83 \cdot 10^{-3}$ 1/s

falls to the brittle to ductile transition and the higher $1.5 \cdot 10^{-2}$ 1/s to completely brittle range. Neither ice failure patterns nor ice loads indicated any significant difference at this velocity range.

The observed narrow line like contact and the mountain ridge shaped solid ice cross section is depicted in Fig. 9a. The ridge is sharper than in some other crushing tests and may be a result of now used snow ice compared to columnar ice that can spall at a blunter angle. The ridge shape is idealized in Fig. 9b for simple average stress distribution calculations. In this simplified geometry the distribution of stress or strain rates changes significantly from those outside the ridge area. An approaching ice crystal within the solid ice is experiencing a cumulatively increasing stress and stress rate while approaching the contact, Fig. 9c. Actually the stress rate or strain

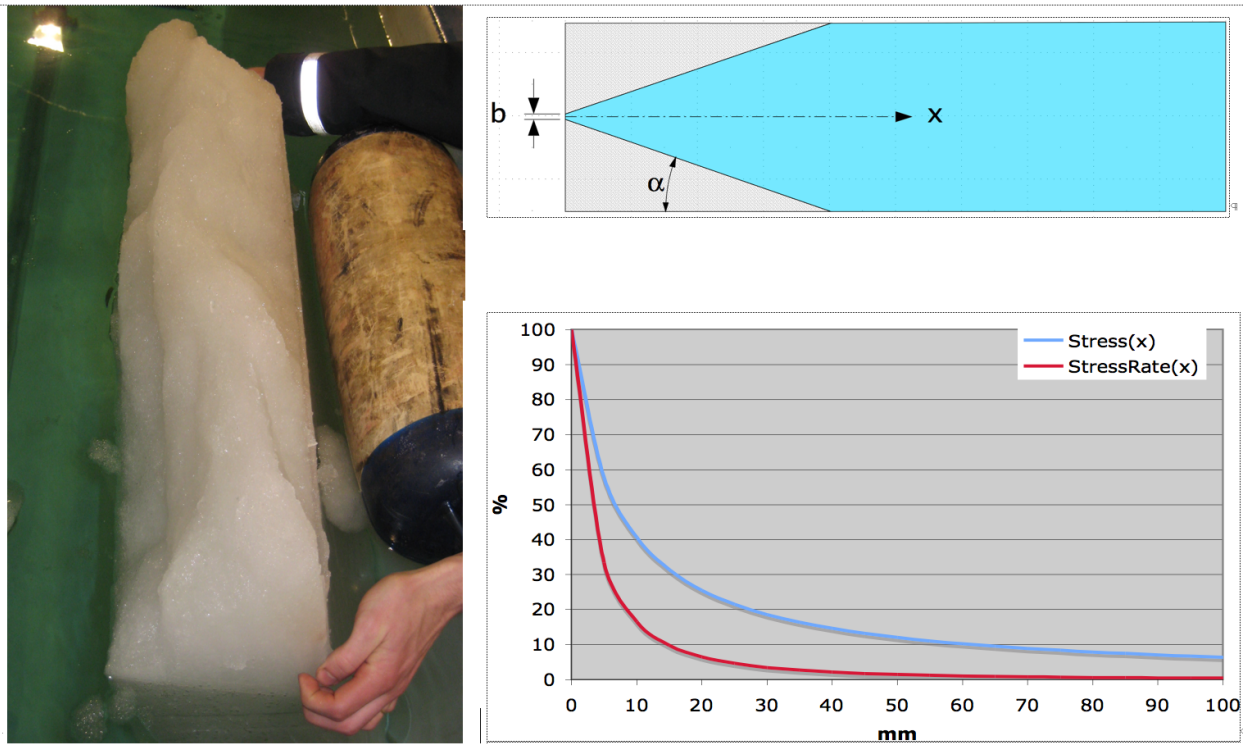

Fig. 9a, Solid ice edge ridge shape, 9b, cross section idealized as a wedge, and 9c, mean stress and stress rate (%) from the maximum at distance x (mm) from the b=5 mm wide contact line inside $2\alpha=40^{\circ}$ solid ice edge

rates are practically zero at a distance farther than about 100 mm ahead of the crushing. E.g., after the 1.02 MPa initial peak in Fig 8, variations occur only in relation to the low average stress level. The average continuous crushing stress at time 52 s (half way between the cursors at the centre, omitting the gradual load build up after a larger load release) is only about 165 kPa with 15 kPa standard deviation while local pressure at line like contact is above 4 MPa, Fig. 8. However close to the solid contact, the average stress and strain rates increase rapidly, Fig. 9c. Hence, the ice behaviour turns from ductile to brittle just in less than about 10 millimetres, or in time space depending on ice velocity, from less than a second to the order of 10 seconds before crushing occurs, e.g. 1,7 seconds in Fig 8. This crude order of magnitude analysis explains how only ice close to the narrow contact line behaves in brittle failure mode and how the ridge shape can persist. The cracks initiated in brittle region will propagate far into the ductile region, chipping (flaking and spalling) solid ice faces continuously in random spots along the contact line and this way maintaining the cross section shape as that of a steep mountain ridge. As local solid ice brittle failures occur randomly starting from highest stress spots – the hot spots – the size scale con-

trolled by contact line width limits also the action radius of a single hot spot initiated crushing/spalling along the contact line.

EFFECT OF PANEL COMPLIANCE IN DESIGN

An unexpected observation in these tests was that the plate compliance had no effect on the crushing pressure distribution against the stiffened plate. Both the initial pressure distribution at the initial peak load and in continuous crushing indicated no difference on the centre stiffener compliance, or plate compliance in between the stiffeners, cf. Fig. 5 and 7. The contact pressure never concentrated on the locations of stiffeners. This finding was evident in all 22 cases in these tests including ductile and brittle ice failure modes, and with the centre stiffener compliance increased for more than two orders of magnitude, cf. Fig. 2. The measured pressure distribution independence of stiffeners is different from the postulated pressure distribution in Fig. 10, Varsta 1983, Riska et al. 2002, which is based on the assumption that ice acting against the reinforced plate behaves like a continuum. This has an analogy to a beam on elastic foundation in which the beam presents the surface plating, stiffeners the supports, and the ice the elastic foundation. Such an assumption will produce higher pressure at the locations of stiffeners.

The present measurement results indicate that the pressure distribution in contact line direction is uncorrelated to the surface plate or reinforcements stiffness distribution. The only effect of softening the centre stiffener was the shift of ice load path to the fixed frame from the centre to the neighbouring stiffeners while the direct crushing pressure distribution remained unchanged. The reason is that ice failure in line like contact has a limited action radius, as explained in the previous Chapter. This radius depends on the width of contact line, typically less than 5 mm in present tests, and/or on the ice crystal size. In crushing tests by Joensuu 1988, and Jordaan 2008, it has been learnt that the crushing – ice failure – starts at small high-pressure contact areas and spreads fast to a wider area. Each independent hot spot crushing isolates the continuum deformation based interaction in its neighbourhood. As such randomly varying actions have no correlation beyond certain range it is impossible for the approaching ice to sense the small deflection of the plate against which it is crushing. A further analysis to find out both the time and spatial correlation of hot spots is planned to find out these correlation ranges, c.f. Taylor, 2010.

If a ship hull or offshore structure surface plating thickness were determined by using the pressure distribution in Fig. 10, the plate thickness would be too thin. The reason is that based on the present measurements the pressure distribution is constant and more of the total load will be acting at the centre section of the free span between the stiffeners. However, dimensioning according to on Fig. 10, the pressure distribution is based on experimentally determined effective pressure values that include the effect of uneven pressure distribution. Hence while the constant pressure distribution is adopted the true experimentally determined constant effective pressure will be lower and the same plate thickness as used earlier will be retained. This is valid e.g. for the Finnish-Swedish Ice Class Rule.

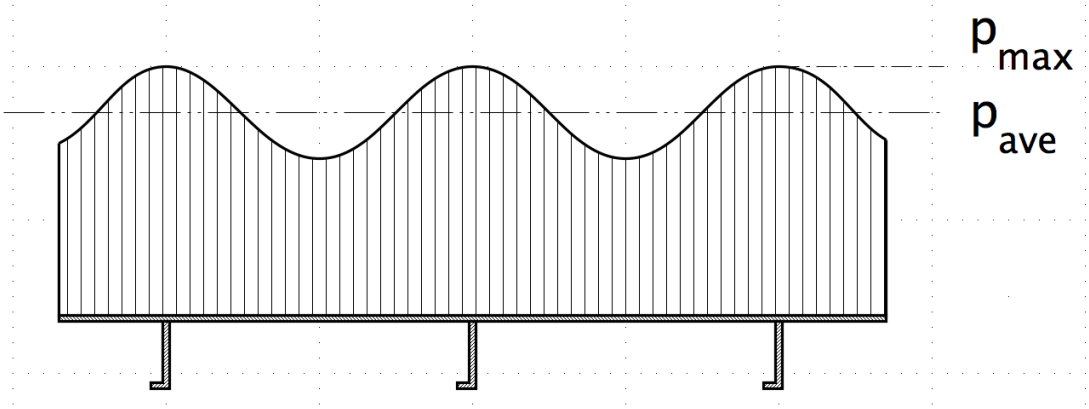

Fig. 10. Crushing pressure according to the assumed ice continuum model.

CONCLUSIONS

Ice crushing laboratory tests were carried through with scale ratio close to the full-scale in order to learn more on structure compliance effects in crushing pressure distributions. A total of 22 ice blocks were crushed at different ice velocities and foundation stiffness distributions.

The model ice was manufactured with snow seeding and vacuum water impregnation in moulds. The produced ice was homogenous, low porosity, and with strength properties scalable close to the geometric scale. The crushing tests with same set-up parameters produced well repeatable results.

A special rig was constructed for fixing the ice block and pushing it at constant pre-selected velocity. The new feature in the test set-up was a target plate in the rig against which the ice was crushing had a plate reinforcement that allowed its stiffness to be adjusted. The target plate was furnished both with a tactile sensor for direct crushing pressure readout, and with strain gauges to determine the ice load path changes in the reinforced plate while the reinforcement stiffness was changed.

The general crushing patterns were similar to what has been learnt from previous crushing tests: initial high peak load after which a significantly reduced and randomly varying ice load in continuous crushing. Both ductile, transition from ductile to brittle and completely brittle ice failure modes were encountered.

The observed ridge shaped solid ice edge profile during continuous crushing, simplified to a wedge model, proves that ice failure behaviour is brittle only at narrow distance from the ice edge contact to the solid object. Beyond the distance scale of contact line width ice behaviour is ductile. Continuous spalling and flaking initiating from the hot spots retains the mountain ridge shaped solid ice edge.

A new finding was that the target plate stiffness distribution played no role in crushing. No crushing pressure concentration occurred at the locations of reinforcements regardless that one stiffener was completely removed with an effective two orders of magnitude reduction in the plate stiffness at that location. The reason for such independence is traced to the limited action radius of randomly starting crushing initiations at hot spots along the narrow contact line.

The results indicate that the ice crushing pressure in the design of plating thickness should be constant regardless of stiffeners. However, this change to those practises assuming higher crushing pressure at reinforcement locations does not have effect to plate thicknesses. The reason is

that empirically determined average and peak pressure values already have inherited higher than true average pressure due to the continuum model based pressure distribution.

ACKNOWLEDGEMENTS
The authors want to express their gratitude to the Finnish Funding Agency for Technology and Innovation (TEKES), Technical Research Centre of Finland (VTT), and the participating Finnish companies Aker Arctic and Technip that made this STRUTSI subtask research possible.

REFERENCES

Finnish-Swedish Ice Class Rules (2002). Bulletin No.13. Finnish Maritime Administration, Helsinki, Finland.

Frederking R., (2004): Ice Pressure Variations During Indentation. Proc IAHR Symposium on Ice. Pp. 307-314, St Petersburg, Russia.

Joensuu, A. (1988): Ice Pressure Measurements using PCDF Film. Proceedings 7th International Conference on Offshore Mechanics and Arctic Engineering (OMAE 1988) Houston, February 7-12, 1988, Vol. IV, p. 153-158

Jordaan I. J., Wells J., Xiao J., and Derradji-Aouat A. (2008): Ice Crushing and Cyclic Loading in Compression. Proc. IAHR Symposium on Ice, Vancouver, Canada.

Lindholm, J.E., Riska, K., Joensuu, A., (1990). Contact between structure and ice; results from ice crushing tests with flexible indentor. Helsinki University of Technology, Ship Laboratory, Report M-101.

Määttänen M., Marjavaara P., Saarinen S., and Laakso M. (2011): Ice crushing tests with variable structural flexibility. *Journal of Cold Regions Science & Technology* (accepted to be published),

Riska K., Uto S., Tuhkuri J. (2002): Pressure distribution and response of multiplate panels under ice loading. Cod Regions Science and Technology. Vol. 34, pp. 209-225.

Sodhi, D. S., Takeuchi, T., Nakazawa, N., and Kawamura, S. A. M. (2001). Measurements of ice force and interfacial pressure during medium-scale indentation tests in Japan. Proc. 16th International Conference on Port and Ocean Engineering under Arctic Conditions, Ottawa, Ontario, Canada, pp. 617-626.

STRUTSI project: http://strutsi.vtt.fi/en/index.htm

Takeuchi, T. , Masaki T., Akagawa S., Kawamura M., Nakazawa N., Terashima T., Honda H., Saeki H. and Hirayama K. (1997). "Medium-Scale Field Indentation Tests (MSFIT) - Ice Failure Characteristics in Ice/Structure Interactions," *Proc. of the 7th Int. Offshore and Polar Engineering Conference,* Vol. II, pp. 376-382, Honolulu, USA.

Taylor, R.S., (2010). Analysis of Scale Effect in Compressive Ice Failure and Implications for Design. PhD Thesis. Memorial University of Newfoundland. St. John's, NL. May 2010.

Varsta P. (1983). On the mechanics of ice loads on ships in level ice in the Baltic Sea, Technical Research Centre of Finland, Esbo, Finland.